Coherent THz Synchrotron Radiation from a Storage Ring with High-Frequency RF System

F. Wang, D. Cheever, M. Farkhondeh, W. Franklin, E. Ihloff, J. van der Laan, B. McAllister, R. Milner, C. Tschalaer, D. Wang, D. F. Wang, A. Zolfaghari, and T. Zwart

MIT-Bates Linear Accelerator Center, Middleton, Massachusetts 01949, USA

G. L. Carr and B. Podobedov

National Synchrotron Light Source, Brookhaven National Laboratory, Upton, New York 11973, USA

F. Sannibale

Lawrence Berkeley National Laboratory, Berkeley, California 94720, USA

(Received 19 October 2005; published 13 February 2006)

The generation of brilliant, stable, and broadband coherent synchrotron radiation (CSR) in electron storage rings depends strongly on ring rf system properties such as frequency and gap voltage. We have observed intense coherent radiation at frequencies approaching the THz regime produced by the MIT-Bates South Hall Ring, which employs a high-frequency S-band rf system. The measured CSR spectral intensity enhancement with 2 mA stored current was up to 10 000 times above background for wave numbers near 3 cm^{-1}. The measurements also uncovered strong beam instabilities that must be suppressed if such a very high rf frequency electron storage ring is to become a viable coherent THz source.

DOI: 10.1103/PhysRevLett.96.064801 PACS numbers: 41.60.Ap, 29.20.Dh, 41.75.Ht

The THz frequency region has been traditionally a difficult portion of the electromagnetic spectrum to access. Since the first report of nonbursting, brilliant, coherent THz radiation detection at BESSY [1], stability of the coherent synchrotron radiation (CSR) flux has become a distinguishing feature of storage ring-based THz sources among other methods of accelerator based THz production. Many scientific applications would benefit from a very stable source of brilliant, broadband CSR [2].

The use of higher rf frequency and voltage to make short bunches for THz CSR generation in an electron storage ring was first proposed in 1994 [3]. Significant progress in understanding storage ring CSR has been made since then [4,5]. It is understood that a higher rf frequency and voltage decreases the bunch length and raises the threshold of bunch intensity for stable CSR operation. High bunch intensity in a short bunch has multiple advantages including quadratic enhancement of the CSR power and extension of the CSR spectrum to higher frequencies (due to a sharper leading edge of the bunch, mainly caused by CSR wakefield). The recently developed CSR generation model [6] agrees well with BESSY II operational results. Also, with higher rf frequency, shorter bunch length could be achieved with a larger first order lattice momentum compaction factor (α), which is typically more suitable for stable ring operation.

However, there are practical limits for the use of high rf frequencies in a storage ring. Higher-order-mode (HOM) and nonlinear fields associated with smaller aperture and cavity volume could severely limit stored beam current and beam lifetime. Also coupled bunch instabilities caused by narrow band impedance from rf cavities could be much worse with higher rf frequency. For these and other technical reasons, most electron storage ring light sources employ rf frequencies of 500 MHz or lower. At present, the MIT-Bates South Hall Ring (SHR) is the only electron storage ring equipped with a single-cavity 2.856 GHz rf system. The SHR has been used primarily for internal target nuclear physics programs. It normally operates with a long bunch length ($\sim$18 ps, rms) and with typical stored current of 200 mA distributed across 1812 bunches. A plan to use the MIT-Bates SHR as a high brilliance THz test source has been presented in Ref. [7].

For an electron bunch to radiate coherently at wavelength λ, its length should be comparable to or shorter than λ. For coherent THz production this implies an rms bunch length below 1 mm. A program of measurements to characterize the potential of the SHR to serve as a THz source began with a test of several low-α lattices. The momentum compaction α, evaluated from measurements of SHR synchrotron frequency as a function of rf voltage, was reduced from 0.024 to 6×10^{-4}. It became increasingly difficult to store beam as the momentum compaction was lowered, particularly for $\alpha < 10^{-4}$ optics. This is one of the main subjects for further exploration.

Bunch length measurements were performed with a Hamamatsu C6860 synchroscan streak camera. Visible synchrotron light from SHR dipole LB9 was brought to the camera by a series of mirrors. Because of present SHR injection system limitations, a uniform fill (electron bunches in every rf bucket) is the only bunch pattern available. Since the camera synchroscan frequency is 81.6 MHz and the CCD integration time used was 111 ms, the bunch length measured was, in fact, the average value for 1/35 of the SHR's 1812 bunches over $\sim 10^5$ turns. The rms bunch length measured for the lowest

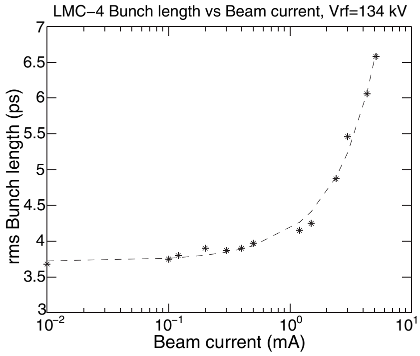

FIG. 1. Measured SHR bunch length from a streak camera vs stored beam current.

α lattice that could stably hold the beam was 3.5 ps. Bunch length measurements taken as a function of stored current (see Fig. 1) show significant lengthening when stored current $I > 2$ mA (1.1 μA/bunch). This is probably due to beam instabilities that result in coherent synchrotron oscillations (to be described below).

During the second run, direct CSR power and spectral measurements were performed using a setup depicted in Fig. 2. Synchrotron radiation emitted from SHR dipole LB16 was extracted through a 9 mrad horizontal and 18 mrad vertical port. It then passed through a 6 mm thick fused quartz viewport, followed by two parabolic reflectors that collected the light and matched it to a spectrometer. The window transmission is more than 50% below 0.5 THz and falls to about 14% at 1 THz (33.3 cm^{-1}). The spectrometer was a commercial Nicolet Magna 860 Fourier Transform Infrared Spectroscopy interferometer with a liquid helium cooled silicon composite bolometer as detector. A sensitive detector was necessary to allow for direct comparison to a thermal source as well as to overcome the rather poor optical throughput of various system components at frequencies below 10 cm^{-1}. Special care was taken to bypass some of the spectrometer's inherent high-pass electronic filters and phase correction algorithms that would otherwise have corrupted the spectral fidelity at such long wavelengths. With this setup, we found that the spectrometer could sense coherent radiation to frequencies as low as 1 cm^{-1}. Figure 3 shows the detected radiation intensity for several CSR emission conditions. Also shown is a background spectral intensity, measured with no beam in the storage ring. This signal is from the 300 K blackbody background and serves as a known source for intensity comparisons. The CSR enhancement with 2 mA beam was up to 10 000 near 3 cm^{-1}. The quadratic dependency of the spectra intensity as a function of beam current is shown in Fig. 4. Above 2 mA, the dependence of intensity on the current is between linear and quadratic, with enhancement (relative to 300 K blackbody radiation) of up to 80 000 with 10 mA stored beam. It should be noted that the intrinsic enhancement is even higher, as the 300 K background is not affected by the throughput limitations of the ring vacuum chamber. We also examined incoherent radiation from long bunches, and found that signals at the same low currents were below the experimental detection limit.

To verify the coherence of the radiation in the low beam current region, spectra were measured with different bunch lengths at a fixed SHR current (2 mA). Figure 5 shows the radiation power spectrum for three different rf gap voltages (i.e., different bunch lengths). Overall radiation intensity decreased by a factor of 300 when the bunch length was increased from 4 to 7 ps rms, thereby confirming that the

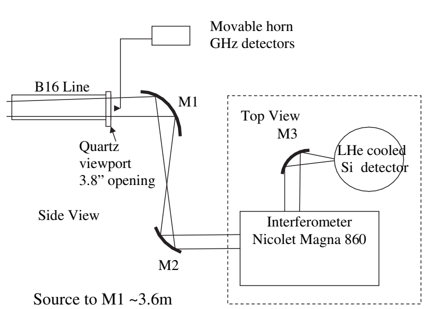

FIG. 2. Measurement setup for the far-infrared radiation.

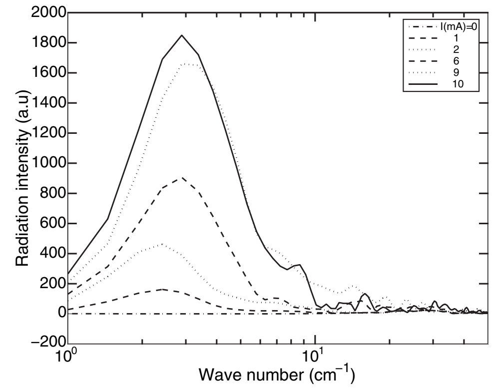

FIG. 3. Radiation power spectra for several SHR currents with fixed rf voltage (134 kV). Gain of interferometer filters: 316, 1.

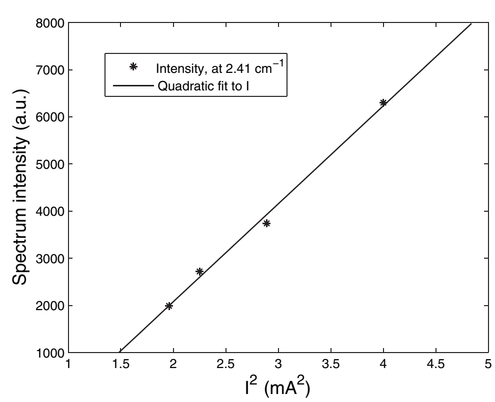

FIG. 4. Quadratic dependency of spectra intensity of CSR to beam current.

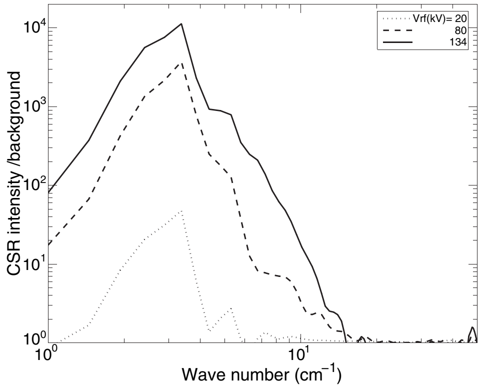

FIG. 5. Intensity ratio of CSR to background for different bunch lengths. $I = 2$ mA. Measured rms bunch length (ps): 7.6, 4.4, 4.0, corresponding to the rf peak voltage Vrf (kV) of 20, 80, and 134.

radiation enhancements were, indeed, due to the shorter bunch length.

Furthermore, the measured spectrum closely resembles the calculated CSR spectra expected from a Gaussian beam. Figure 6 shows the ratio of the CSR intensity to the background as a function of wave number for three SHR beam currents. Also shown is a calculated ratio of CSR radiation from a Gaussian beam of 3.5 ps rms bunch length to incoherent radiation, all with 2 mA average current. It is noticed that the incoherent radiation intensities were lower compared to measured background signals and no corrections have been made to account for the transmission of the quartz window. Therefore the measured ratio in Fig. 6 should be lower compared to the calculated ratio. The level of agreement confirms that at low stored current, the CSR is produced by bunches of Gaussian distribution with little distortion.

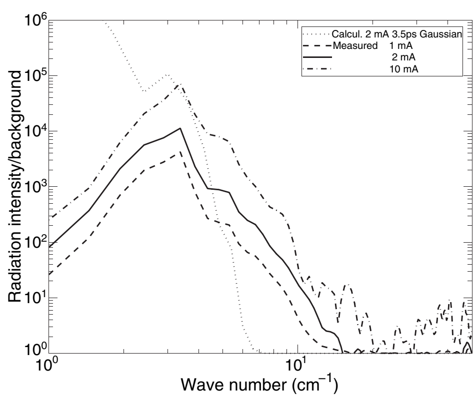

FIG. 6. Intensity ratio of power spectra of radiation to background. Calculated ratio of CSR from 2 mA beam of bunch length 3.5 ps rms with Gaussian distribution to incoherent radiation of the same current. The humplike shape on the calculated spectrum indicates significant shielding from the vacuum chamber (two plates approximately [12]).

Another important issue is to distinguish between steady-state and bursting mode due to microbunching instabilities as observed in other rings [8,9]. The calculated bunch intensity threshold of microbunch instability [5,6] is about 40 μA/bunch for $\sigma \sim 3.5$ ps, much higher than the measured bunch "lengthening" threshold of 1.1 μA/bunch. However, the CSR spectra for currents above the observed lengthening threshold still exhibit distinct peaks close to those observed with the 3.5 ps bunch length Gaussian beam and display a larger radiation power than the increased bunch length would suggest. It is likely that a partially coherent state has been achieved in which the bunch length measured by the streak camera is lengthened by a bunch longitudinal oscillation. At higher currents, the portion of the bunch maintained in a tight longitudinal distribution could be distorted due to CSR and exhibit some oscillations. The radiation from these electrons would dominate the power spectra, while the rest of the particles were spread out in wider longitudinal phase space, which did not contribute much to the power spectra. In fact, because of the short lifetime of the beam at higher current ($\sim$5 minutes), to ease the measurements of the spectra (takes minutes to scan), the ring was under "top-off" injection mode. The injected beam had a very long bunch length ($\sim$30 ps FWHM) after traversing an energy compression system downstream of the injection linac. The radiation spectra were not altered due to continuous injection.

The radiation signals in the time domain revealed more beam instability phenomena. To examine the time structure of the CSR we utilized experimental techniques developed earlier for the NSLS vacuum ultraviolet (VUV) ring [10]. Specifically, synchrotron radiation in the mm range was collected by a microwave horn followed by a matching detector. Two independent systems, sensitive in the 50–75 and 75–110 GHz ranges, respectively, were used. Each was attached to a movable mount located immediately after the quartz viewport and upstream of the bolometer. The signals were ac coupled to a digital oscilloscope, so that only variations in the radiation flux were recorded. When stored beam current was below 2 mA, some degree of "bursting" was observed with a period of 200 ms [see Fig. 7(a), peaks of the traces], a time interval equivalent to the transverse synchrotron radiation damping time of the SHR. When stored current was raised above the 2 mA threshold, the bursting period fell to 100 ms, the longitudinal synchrotron radiation damping time of the ring [Fig. 7(b)]. The onset of higher frequency bursting was coincident with the bunch lengthening shown in Fig. 1, and indicates that the bunch had developed longitudinal instabilities. As mentioned above, the bunch intensity was still far below the CSR driven microbunching instability threshold. Therefore the bursting addition and lengthening here are more likely caused by ring impedance-dependent single or coupled bunch longitudinal instabilities as observed in the NSLS

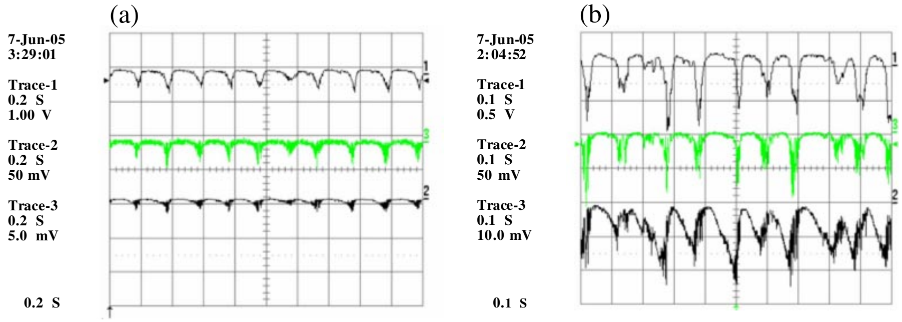

FIG. 7 (color online). (a) Bolometer detector and microwave detector signals. Trace 1: bolometer; trace 2: 75–110 GHz detector; trace 3: 50–75 GHz detector. $I \approx 2$ mA. Bursting period: ~200 ms. (b) $I \approx 10$ mA. Bursting period: ~100 ms.

VUV ring [11], except the basic bunch length here is short enough to produce stable CSR in the sub-THz region. Current-dependent longitudinal beam instabilities were also observed in bunch shape measurements from the streak camera. The streak camera usually took a sequence of 100 images of the beam, each covering a 111 ms integration period. At low current, consecutive profiles of the beam displayed little variation. At higher current, distortion of the distribution showed up and varied from profiles, as shown in Fig. 8.

In summary, for the first time, tests were performed on CSR generation in a storage ring with an S-band rf frequency system. The studies demonstrated that 1-mm bunch length can be obtained with a moderately low-α (6×10^{-4}) lattice. Intense radiation was detected, which was clearly coherent with beam current ≤ 2 mA (corresponding bunch intensity 1 μA). Suppressing beam instabilities (probably dominantly multibunch instability at present) emerged as the first challenge in pursuing a very brilliant stable storage-ring-based THz CSR source employing a high-frequency rf system. A few technical adjustments are crucial to address this issue. These include implementation of bunch-to-bunch filling injection mode to allow studies of single or multibunch instabilities and bunch lengthening mechanisms, installation of a ferrite-loaded HOM absorber around the rf cavity to suppress HOM from the rf cavity, etc.

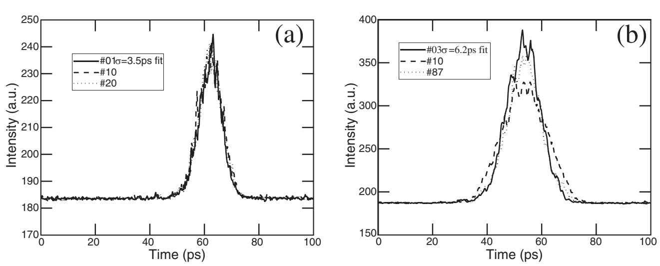

FIG. 8. (a) Three bunch profiles from streak camera at $I = 0.09$ mA. Each profile was the average of many bunches over $\sim 10^5$ turns. (b) Typical variation in bunch profiles at $I = 5.1$ mA.

The tests described were made possible by the support of MIT and the U.S. Department of Energy, Office of Nuclear Physics. BNL/NLSL provided key instrumentation and expertise for bunch length and CSR measurements.

[1] M. Abo-Bakr *et al.*, Phys. Rev. Lett. **88**, 254801 (2002).
[2] E. J. Singley *et al.*, Phys. Rev. B **69**, 092512 (2004).
[3] J. B. Murphy and S. Krinsky, Nucl. Instrum. Methods Phys. Res., Sect. A **346**, 571 (1994).
[4] K. Bane *et al.*, in *Proceedings of the Micro Bunches Workshop, Upton, NY, 1995*, edited by E. B. Blum *et al.*, AIP Conf. Proc. No. 367 (AIP, New York, 1996), p. 191.
[5] G. Stupakov and S. Heifets, Phys. Rev. ST Accel. Beams **5**, 054402 (2002).
[6] F. Sannibale *et al.*, Phys. Rev. Lett. **93**, 094801 (2004).
[7] F. Wang *et al.*, in *Proceedings of the 2005 IEEE Particle Accelerator Conference, Knoxville, TN* (IEEE, Piscataway, NJ, 2005), p. 3783.
[8] J. M. Byrd *et al.*, Phys. Rev. Lett. **89**, 224801 (2002).
[9] M. Abo-Bakr *et al.*, in *Proceedings of 2003 IEEE Particle Accelerator Conference, Portland, OR* (IEEE, Piscataway, NJ, 2003), p. 3023.
[10] B. Podobedov *et al.*, in *Proceedings of the 8th European Particle Accelerator Conference, Paris, France, 2002* (EPSIGA and CERN, Geneva, 2002), p. 1553.
[11] G. L. Carr *et al.*, Nucl. Instrum. Methods Phys. Res., Sect. A **463**, 387 (2001).
[12] S. A. Kheifets and B. Zotter, CERN Report No. SL-95-92(AP).